Paper No. 67. (quote when citing this article)
Eleventh World Conference on Earthquake Engineering
ISBN: 0 08 042822 3

11 WCEE

SYSTEM IDENTIFICATION OF THE HUALIEN LSST MODEL STRUCTURE

TOSHIO KOBAYASHI, HIROYOSHI YAMAYA
Kajima Technical Research Institute, Kajima Corporation , 19-1, Tobitakyu 2-Chome, Chofu-shi, Tokyo, 182, Japan

EIJI KITAMURA
Kajima Information Processing Center, Kajima Corporation, 2-7, Motoakasaka 1-Chome, Minato-ku, Tokyo,107, Japan

TATSUYA SUGIYAMA
Engineering Research & Development Division, Tokyo Electric Power Company
4-1 Egasaki-Cho, Tsurumi-Ku, Yokohama, Kanagawa 230, Japan

ABSTRACT

This paper discusses forced vibration tests conducted on a 1/4-scaled nuclear reactor containment soil-structure interaction system by using an exciter, and simulation analyses. For both NS and EW excitations, components orthogonal to the exciting directions were fairly large because of inhomogeneity of the supporting soil. In order to clarify the phenomena, the concept of "Principal Axes (D_1, D_2)" was introduced for the SSI system, and tests results were transposed to the principal axis directions so that the orthogonal components disappeared. The correlation analyses for the tests were carried out using the "Lattice Model", which was able to estimate the variation in soil-structure interaction effects with embedment. Prior to this correlation analysis, the structural properties were revised to adjust the calculated fundamental frequency in the fixed base condition to that derived from the test results. The correlation analysis results coincided well with the test results and it is concluded that the mathematical soil-structure interaction model established by the correlation analysis is efficient in estimating the dynamic soil-structure interaction effect with embedment.

KEYWORDS

Soil-Structure Interaction, Nuclear Power Plant, Forced Vibration Test, Backfill, System Identification, Soil Inhomogeniety, Principal Axis

1 INTRODUCTION

A Large-Scale Seismic Test (LSST) Program (Tang *et al.*, 1991) was conducted at Hualien (stiff soil site), Taiwan, to obtain earthquake-induced soil-structure interaction (SSI) data. This study was undertaken as an extension to the same kind of program conducted at Lotung (soft soil site). Before starting earthquake observations, forced vibration tests using an exciter were conducted to obtain basic dynamic characteristics of the soil-structure interaction system. Two tests were performed: (1) a Forced Vibration Test without embedment (FVT-1) (Morishita *et al.*,1993) and (2) the same test with embedment (FVT-2) (Sugawara *et al.*, 1995). A Photograph and a section of the model structure are shown in Fig. 1 and Fig. 2, respectively.

2 TEST RESULTS

Figs. 3 and 4 show the horizontal displacement orbits of FVT-1 for NS-EW and principal axis (D_1, D_2) direction excitations at the roof, respectively. In Fig.3, each orbit is elliptical. At 4.1 Hz, the D_1 component is predominantly large and the D_2 component is also fairly large. At 4.6 Hz, the D_2 component is predominantly large and the D_1 component is also fairly large. These phenomena are reflected in the resonance curves shown in Fig. 5, which

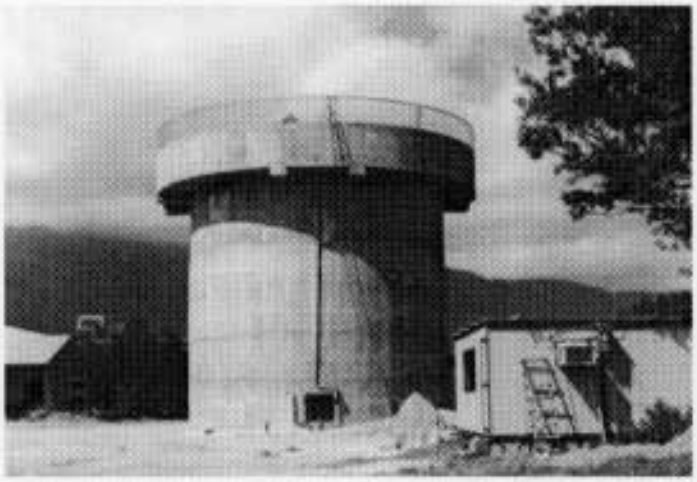

Fig. 1 Photograph of the model structure

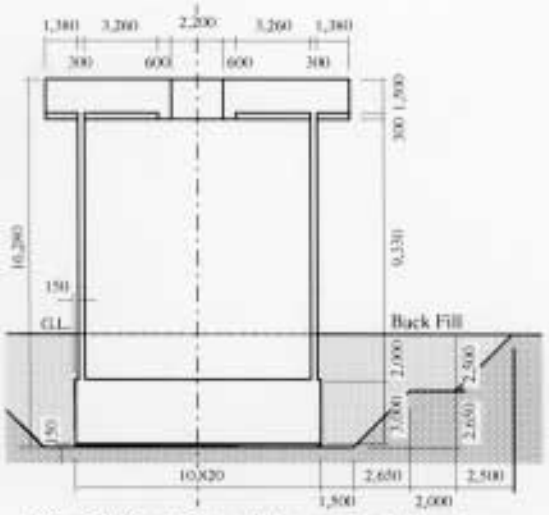

Fig. 2 Section of the model structure

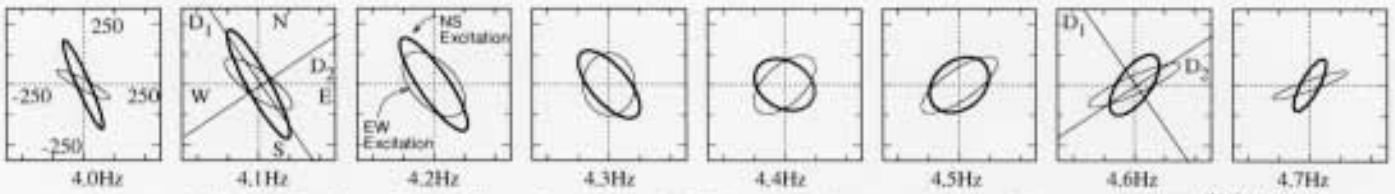

Fig. 3 Orbit of roof floor for NS and EW excitation at roof (without backfill) (Unit:μm/ton)

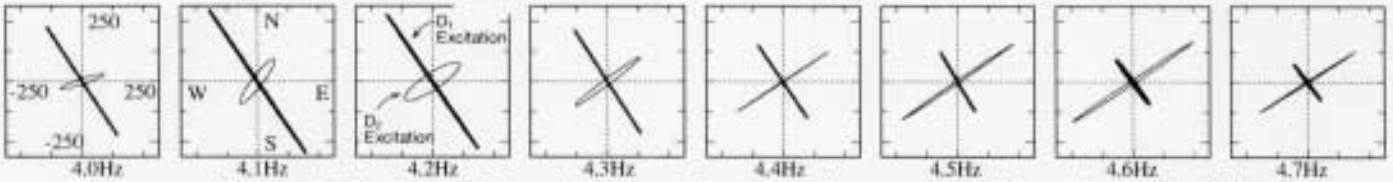

Fig. 4 Orbit of roof floor for D_1 and D_2 excitation at roof (without backfill) (Unit:μm/ton)

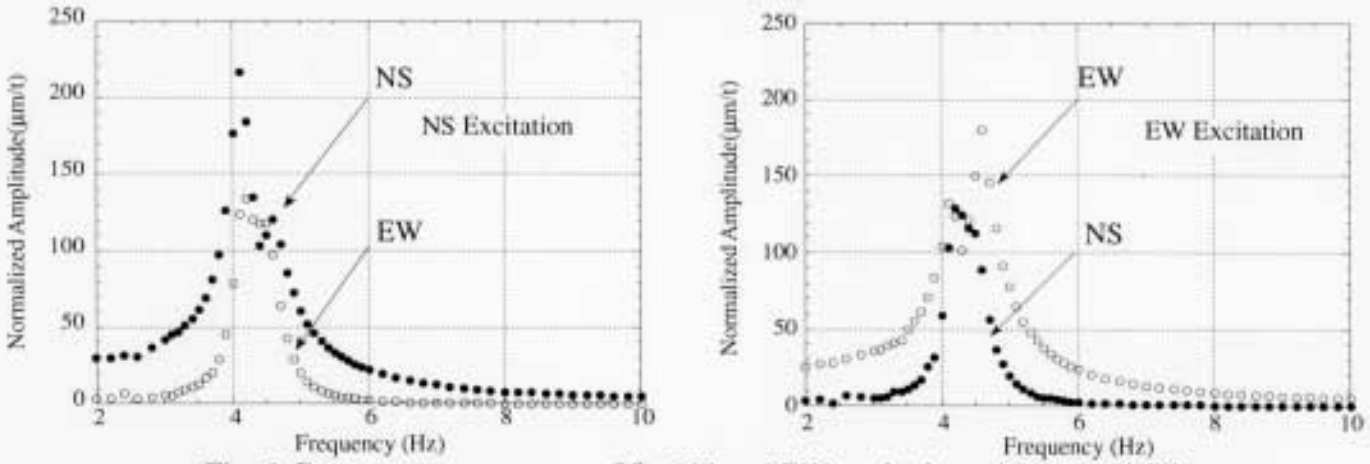

Fig. 5 Resonance curves at roof for NS and EW excitation without backfill

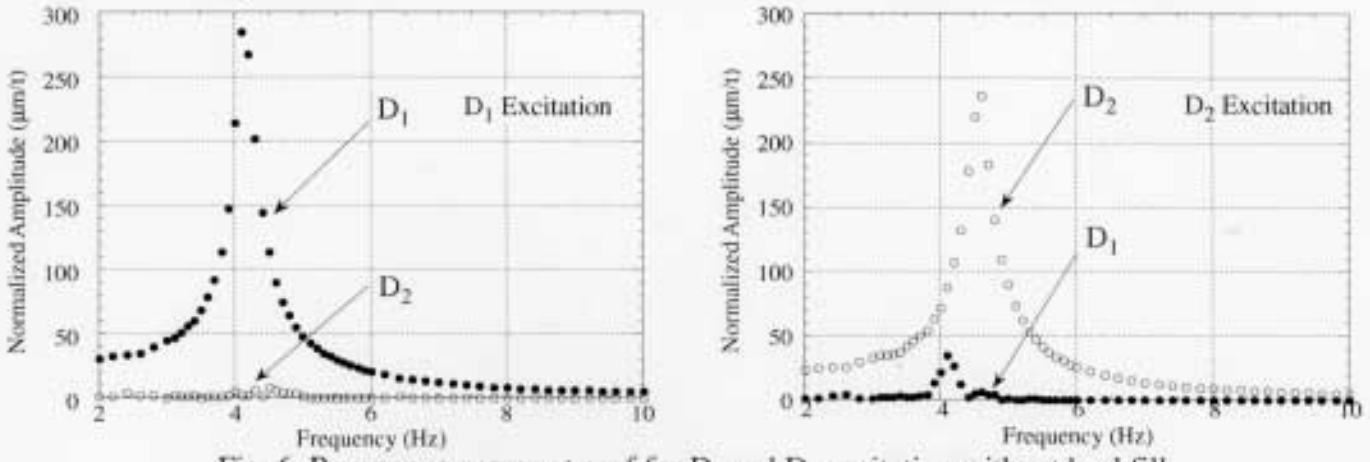

Fig. 6 Resonance curves at roof for D_1 and D_2 excitation without backfill

have two peaks, at 4.1 Hz and 4.6 Hz. The components orthogonal to the exciting directions are about 60% of those in the exciting direction. Fig. 4 is similar to Fig. 3, but Fig. 4 is the result of transposing Fig. 3 to the principal axis directions, D_1 and D_2. Each orbit is almost a straight line and the components orthogonal to the exciting direction are negligible. The resonance curves shown in Fig.6 for D_1 and D_2 excitations have single peaks at 4.1 Hz and 4.6 Hz, respectively. The components orthogonal to the exciting directions are also negligible. Figs. 7~10 are similar to Figs. 3~6, but are for FVT-2. Fig. 9 shows resonance curves for NS and EW excitations where the components orthogonal to the exciting directions are about 20% of those in the exciting directions. Fig. 10 shows resonance curves for principal axis excitation, in which the orthogonal components are negligible. This means that the responses for D_1 and D_2 excitations are not coupled to each other. The angles of the principal axis counterclockwise from plant north direction are obtained as 34° without embedment and 30° with embedment by an eigen value analysis for a variance-covariance matrix (Sugawara *et al.*,1995).

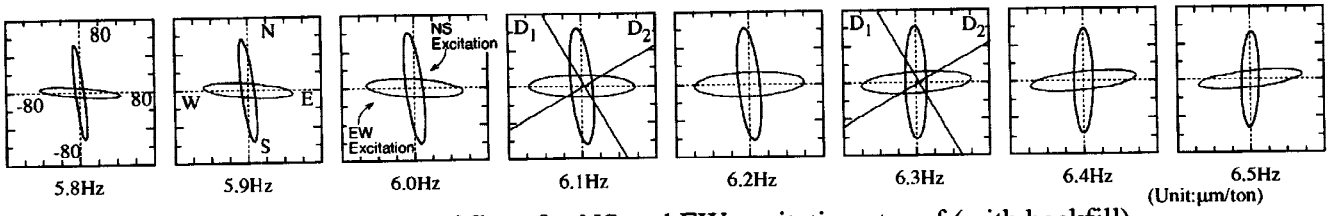

Fig. 7 Orbit of roof floor for NS and EW excitation at roof (with backfill)

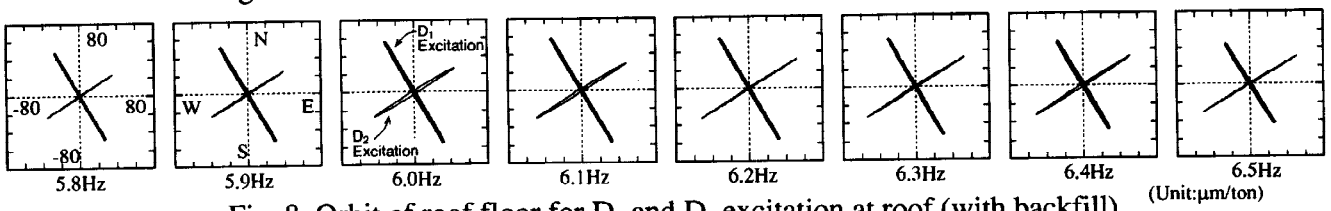

Fig. 8 Orbit of roof floor for D_1 and D_2 excitation at roof (with backfill)

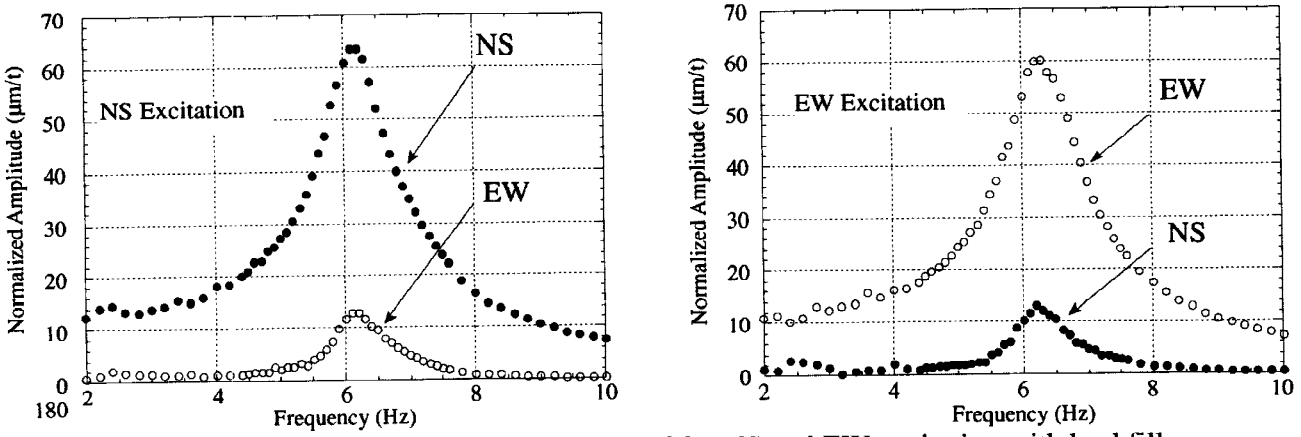

Fig. 9 Resonance curves and orbits at roof for NS and EW excitation with backfill

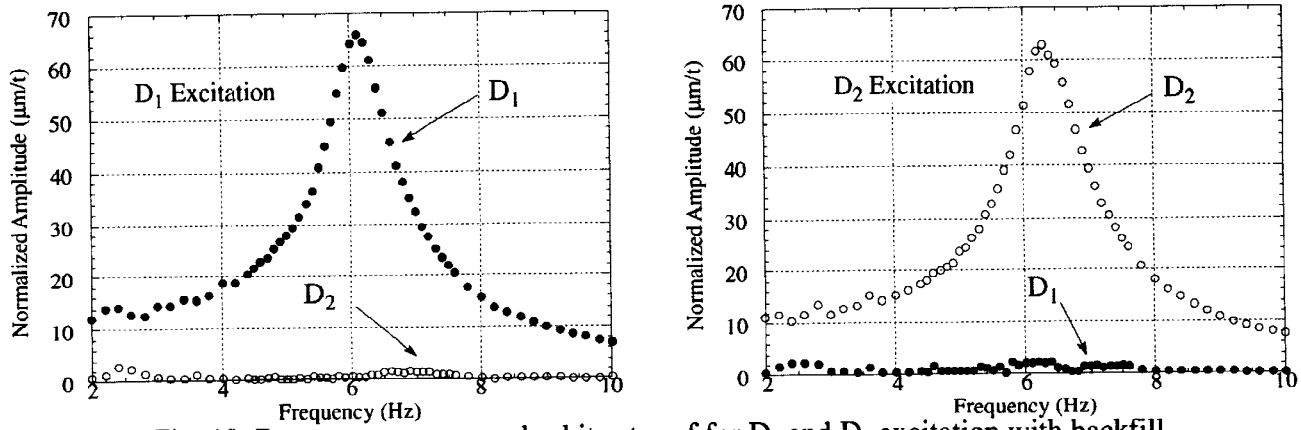

Fig. 10 Resonance curves and orbits at roof for D_1 and D_2 excitation with backfill

The reason why the dynamic characteristics of this cylindrical soil-structure system are not axi-symmetric was considered to be the inhomogeneity of the supporting soil (Sugawara *et al.*,1995) and this was confirmed by the simulation analysis (Yoshida, 1995). Based on these transformed results, peak frequencies, damping factors and displacement component ratios (sway, rocking and elastic deformation of the structure) at the roof floor in the fundamental mode shapes are obtained as shown in Table 2.

3 DYNAMIC CHARACTERISTICS OF MODEL STRUCTURE

3.1 Dynamic characteristics with fixed base condition

The dynamic characteristics of the model structure with the fixed base condition were derived from forced vibration test results by a system identification method (Ishibashi *et al.*, 1994). These results yielded pure structural characteristics which exclude soil-structure interaction effects.

For first floor excitation, the dynamic equation of motion for sway (z), rocking (θ) and elastic deformation (x) is given as EQ (1) and the elastic deformation vector (x) is expressed by EQ (2).

$$M(\ddot{x}+I\ddot{z}+H\ddot{\theta})+C\dot{x}+Kx=0, \quad x=\sum_{j=1}^{N} X_j q_j \qquad (1), (2)$$

where M, C, K are mass, damping and stiffness matrices and I and H are unit and height vector, respectively. X_j is the j-th mode vector and q_j is the j-th time function. Multiplying by the transposed first mode vector from the left side and considering the orthogonal condition for different mode vectors, the dynamic equation of motion of the first mode is given by :

$$X_1^T M X_1 \ddot{q}_1 + X_1^T M I \ddot{z} + X_1^T M H \ddot{\theta} + X_1^T C X_1 \dot{q}_1 + X_1^T K X_1 q_1 = 0. \qquad (3)$$

The following expressions are then introduced for simplicity.

$$\bar{\omega}^2 = \frac{X_1^T K X_1}{X_1^T M X_1}, \; 2h\bar{\omega} = \frac{X_1^T C X_1}{X_1^T M X_1}, \; \alpha = \frac{X_1^T M I}{X_1^T M X_1}, \; \gamma = \frac{X_1^T M H}{X_1^T M X_1}. \qquad (4)$$

Furthermore, time functions are expressed as :

$$q_1 = Q e^{i\omega t}, \quad z = Z e^{i\omega t}, \quad \theta = \Theta e^{i\omega t}. \qquad (5)$$

Applying these expressions to EQ (3), the first mode response of the elastic deformation component for sway and rocking input motion can be derived as :

$$Q = \frac{\omega^2(\alpha Z + \gamma\Theta)}{\bar{\omega}^2 - \omega^2 + 2ih\omega\bar{\omega}} \qquad (6)$$

The dynamic equation of motion with only elastic deformation (fixed base condition) is given by EQ (7) and elastic deformation vector $\bar{x}$ is given by EQ (8).

$$M(\ddot{\bar{x}}+I\ddot{z}_0)+C\dot{\bar{x}}+K\bar{x}=0, \quad \bar{x}=\sum_{j=1}^{N} X_j \bar{q}_j \qquad (7), (8)$$

where $\bar{q}_j$ is the j-th time function. Multiplying by the transposed first mode vector from the left side, and considering the orthogonal condition for different mode vectors, the dynamic equation of motion of the first mode is given by :

$$X_1^T M X_1 \ddot{\bar{q}}_1 + X_1^T M I \ddot{z}_0 + X_1^T C X_1 \dot{\bar{q}}_1 + X_1^T K X_1 \bar{q}_1 = 0 \qquad (9)$$

Applying EQs (4), (5) to EQ (9), it is concluded that the first mode response of the elastic deformation component of the dynamic system with only elastic deformation (fixed base condition) for unit base sway acceleration input (=1) is given by :

$$\bar{Q} = \frac{-\alpha \ddot{z}_0(=1)}{\bar{\omega}^2 - \omega^2 + 2ih\omega\bar{\omega}} \tag{10}$$

Comparing EQ (6) and EQ (10), the first mode response of the elastic deformation component ($\bar{Q}$) with fixed base condition for unit base sway acceleration input is given by the first mode response of the elastic deformation component (Q) of the dynamic system with sway, rocking and elastic deformation for sway and rocking input motion as follows :

$$\bar{Q} = Q \times \frac{-\alpha \ddot{z}_0(=1)}{\omega^2(\alpha Z + \gamma\Theta)} = Q \times \frac{-\alpha}{\omega^2(\alpha Z + \gamma\Theta)} \tag{11}$$

3.2 Mathematical model of structure

The mass matrix and the height vector of the model structure are evaluated from design drawing geometry as shown in Fig.13. The mode shape for the elastic deformation component is represented by the ratio of rotational angle (θ) to horizontal displacement (u) at the roof floor (RF). The observed mode ratio (θ/u) derived from the test results is shown in Fig.11. It is nearly equal to 5.5×10^{-4} rad./cm except in the frequency range below 5Hz, which is used as a first mode vector of elastic deformation (X_1) by interpolating at each mass point. Using these data, values of α and γ defined by EQs (4) are obtained. From EQ (11), resonance curves for fixed base condition ($\bar{Q}$) are obtained by applying measured sway (Z), rocking (Θ) and elastic deformation resonance curves (Q). An example of a resonance curve for fixed base condition derived from the test results after backfill is shown in Fig.12, in which the regression result for the one-degree-of-freedom resonance curve is also shown. Natural frequencies and damping factors obtained by the regression method are summarized in Table 1. With first floor excitation, the averaged test results for natural frequency and damping factor are 9.54 Hz and 1.0 %, respectively.

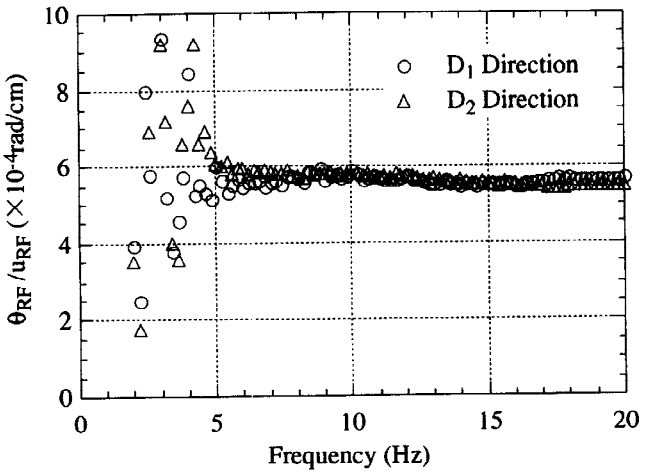

Fig. 11 Observed mode ratio (θ/u) derived from test results

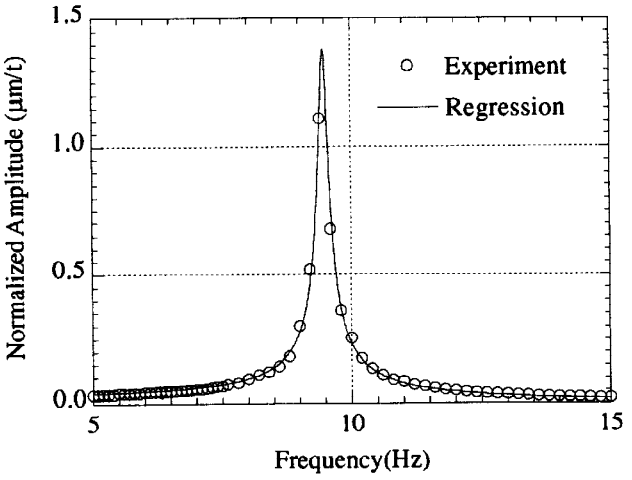

Fig. 12 Resonance curves for fixed base condition (D_1 direction)

Table 1 Regrresion Results

	Test Results				Fixed Base Condition			
	FVT-1		FVT-2		FVT-1		FVT-2	
Direc-tion	f_0 (Hz)	h (%)	f_0 (Hz)	h (%)	f_{f0} (Hz)	h_f (%)	f_{f0} (Hz)	h_f (%)
D_1	4.2	3.6	6.5	8.6	9.42	0.9	9.47	1.0
D_2	4.6	3.7	6.6	8.1	9.56	0.4	9.71	1.8

(f_0: Peak Frequency, h : Damping factor)
Average: f_0 = 9.54 Hz, h_f = 1.0 %

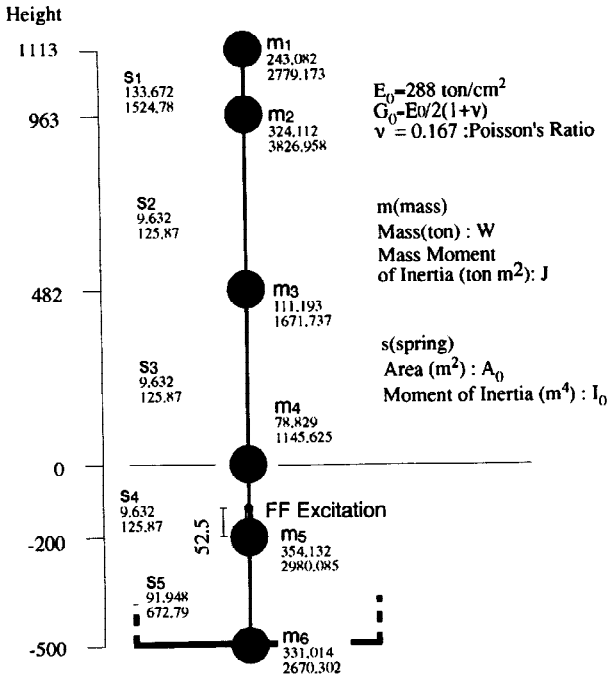

Fig. 13 Lumped mass model

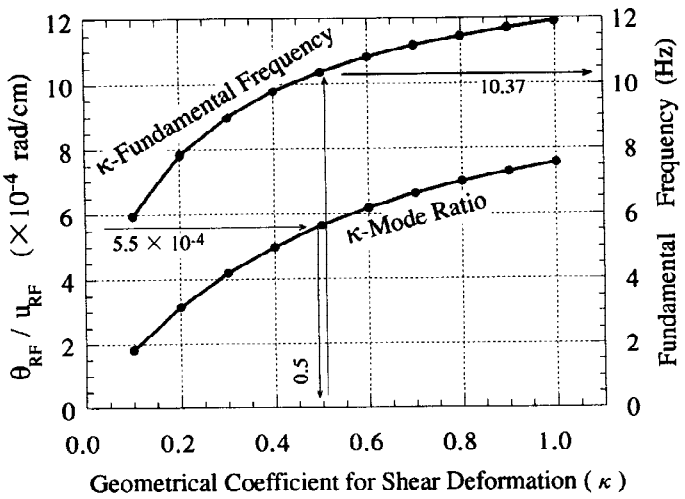

Fig. 14 Relations between geometrical coefficient for shear deformation and mode ratio (θ/u), fundamental frequency

Mode ratio (θ/u) calculated from the flexural and shear beam model is shown in Fig.13, in which the geometrical coefficient for shear deformation (κ) is considered as a parameter. A mode ratio of 5.5 × 10^{-4} rad./cm is derived from this figure, when the geometrical coefficient for shear deformation (κ) is roughly equal to 0.5.

Calculated fundamental frequency for the fixed base condition is shown in Fig.14, in which Young's modulus is considered to be E_0 = 288 ton/cm^2 (which was proposed by the Technical Management Committee of the Hualien Project from the cylinder test results), and the geometrical coefficient for shear deformation (κ) is considered as a parameter. From this figure, the fundamental frequency is 10.37 Hz when the geometrical coefficient for shear deformation (κ) is equal to 0.5.

To adjust the calculated fundamental frequency (10.37Hz) to that derived from the test results (averaged to 9.54Hz) as aforementioned, Young's modulus is revised to effective Young's modulus (Ee) using an apparent stiffness reduction factor (η) as follows :

$$Ee = \eta \times E_0 = 0.85 \times 288 \text{ ton/cm}^2 = 243 \text{ ton/cm}^2$$

$$\eta = (9.54 \text{ Hz} / 10.37 \text{ Hz})^2 = 0.85$$

The reasons for the stiffness reduction effect are considered to be follows :

(1) Concrete material properties of the structure are different from those of the test specimen.
(2) As-built geometry is different from that of the design drawings.
(3) Stress transfer mechanism is different from that of an idealized shell wall because of the complicated construction process.

However, it is difficult to discuss quantitative participation values of these effects on η.

4 CORRELATION ANALYSIS FOR FORCED VIBRATION TEST

4.1 Analytical model

There are many soil-structure interaction analysis models. One that has been used, or will be used in the near future, for aseismic design of commercial nuclear power plants should be selected. The Lattice Model is selected

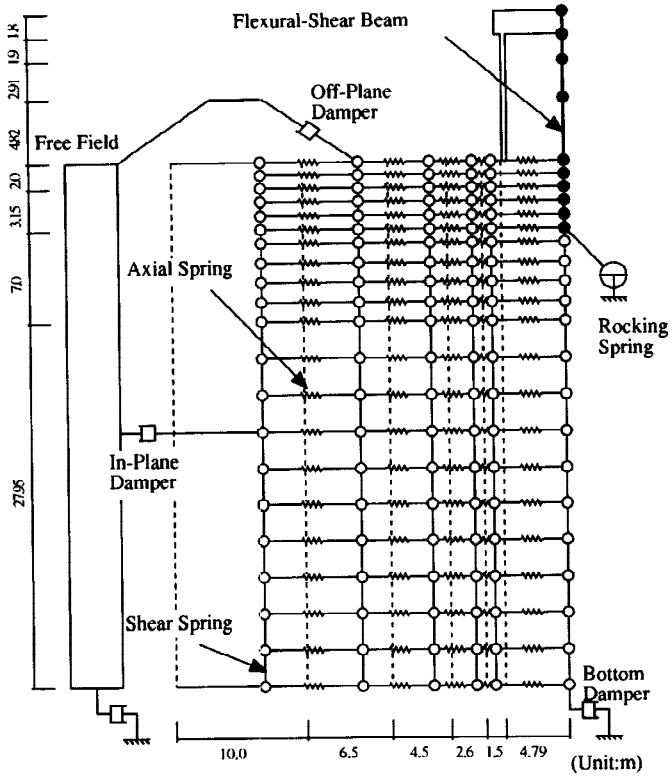

Fig. 15 Analytical model (Lattice model)

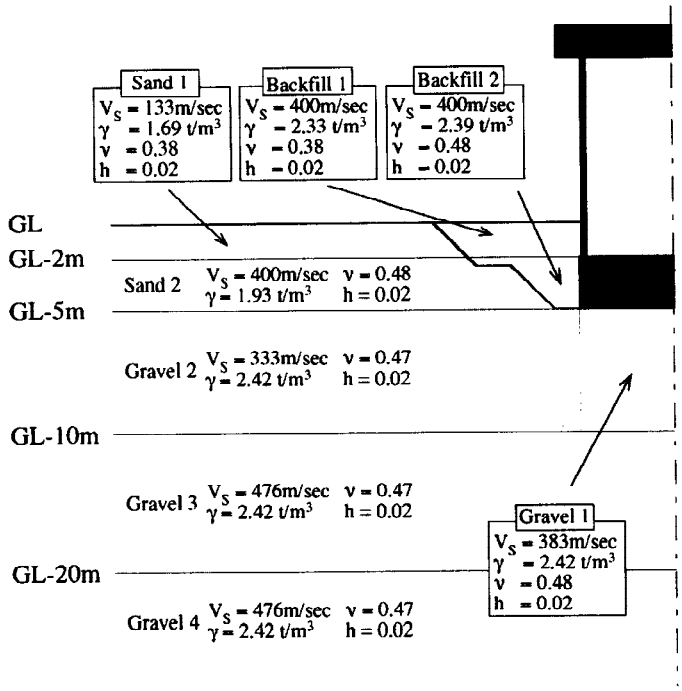

Fig. 16 Soil property

here for the correlation analysis of the forced vibration test for horizontal excitation after backfilling. The input data of the model structure and the general concept of the Lattice Model are shown in Fig.15 and Fig.16, respectively. The revised stick model of the structure established in previous chapter was used.

Unified physical constants of soil for the simulation analysis shown in Fig.16 were proposed by the Technical Management Committee of the Hualien Project as soil input data. These constants were employed directly in the D_1 direction correlation analysis. D_1-Equivalent rocking stiffness ($K_{RR}[D_1]$) was obtained from an axi-symmetric FEM model under supporting layer (GL-5.15m). The rocking stiffness of the supporting soil for the D_2 direction is derived from that of the D_1 direction ($K_{RR}[D_2] = K_{RR}[D_1] \times 1.20$) in consideration of the rocking stiffness of the supporting layer obtained from the test results (Sugawara *et al.*, 1995).

4.2 Correlation analysis results

Calculated resonance and phase lag curves for the D_1 and D_2 directions for first floor horizontal excitation are shown with the test results in Figs. 17. Calculated peak frequencies, damping factors, peak amplitudes and deformation ratios are summarized and compared with the test results in Table 2. The calculated results correlate well with the test results.

Table 2 Calculation results for horizontal excitation at first floor

	Peak frequency (Hz)	Damping factor (%)	Peak amplitude (μm)	Deformation ratio (%)		
				Sway	Rocking	Elastic deformation
Calculation(D_1)	6.41	8.2	10.9	4.2	55.1	40.7
Test result(D_1)	6.5	8.6	9.7	5	55	40
Calculation(D_2)	6.38	8.3	9.9	4.4	51.1	44.5
Test result(D_2)	6.6	8.1	10.4	6	48	46

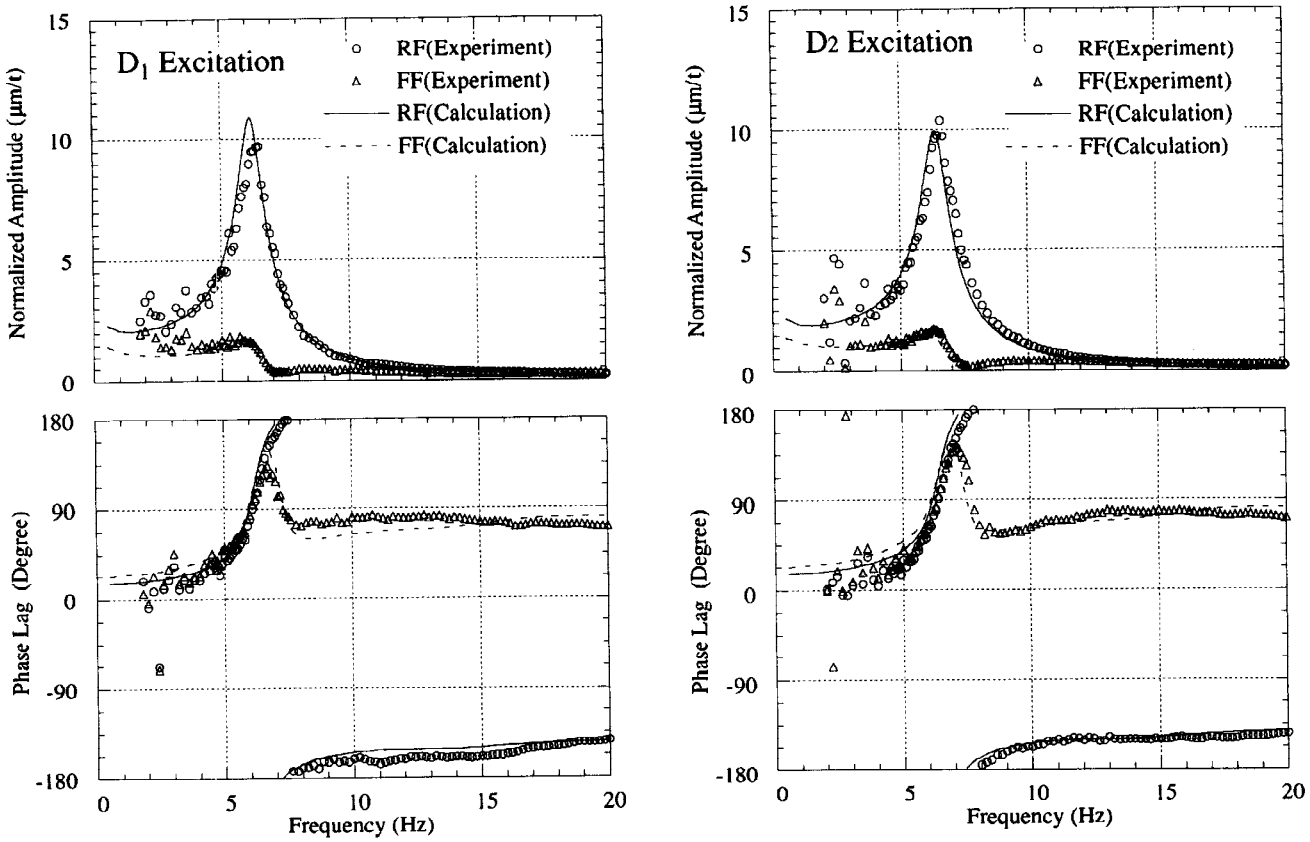

Fig. 17 Resonance and phase lag curves for horizontal excitation at first floor

5 CONCLUSIONS

Concluding remarks obtained from the analysis results are summarized as follows ;

1. The responses for the NS and EW directions were coupled with each other, but they were decoupled by transposing to principal axes (D_1, D_2) excitation.
2. The dynamic characteristics of the model structure with the fixed base condition are derived from test results, and its mathematical model was revised.
3. The results of the correlation analysis coincide well with the test results for peak frequency, damping factor, peak amplitude and deformation ratios (sway, rocking and elastic deformation).
4. The mathematical model discussed in this paper is efficient for estimating a dynamic soil-structure interaction effect with embedment.

REFERENCES

Ishibashi, T. and Naito, Y. (1994). System identification methods of buildings considering rocking motion of the base. *Annual Report, KAJIMA Technical Research Institute:* Vol. 42.

Morishita, H., Tanaka, H., Nakamura, N., Kobayashi, T., Kan, S., Yamaya, H. and Tang, H.T. (1993). Forced vibration test of the Hualien large scale SSI model. *Proc. 12th SMiRT:* K02/1. Stuttgart, Germany.

Sugawara, Y., Uetake, T., Kobayashi, T. and Yamaya, H. (1995). Forced vibration test of the Hualien large scale SSI model (Part 2). *Proc. 13th SMiRT:* KA05/1. pp. 109-114. Port Alegre, Brazil.

Tang, H. T. et al. (1991). The Hualien large-scale seismic test for soil-structure interaction research. *Proc. 11 th SMiRT:* K04/4. Tokyo, Japan.

Yoshida, K. (1995). Fundamental studies on soil-structure interaction problems, *Doctorial thesis.*